in the WLAN and WiMAX frequency bands; however, its sensitivity degrades at higher frequencies. The *E*-plane radiation pattern is bidirectional at the various frequencies.

4. CONCLUSION

A novel UWB dual-band microstrip antenna is presented whose notch bands centered at WLAN and WIMAX can be electronically reconfigured on an individual bases. The technique uses defected ground-plane slit structures with pairs of PIN diodes which are integrated directly onto the antenna's structure. The other advantage is that PIN diodes do not require dc bias lines etched onto the antenna itself, thus avoiding associated problems of dc effects. The antenna is fed with a coplanar waveguide etched on one side of the dielectric structure. The antenna was fabricated on a conventional dielectric substrate with dimensions of 28×30 mm^2. It is shown that individual band limited notches can be separately controlled without affecting each other's or the antenna's UWB performance. In addition, the antenna radiates omnidirectionally in the *H*-plane. The antenna's configuration is simple to manufacture with low cost.

ACKNOWLEDGMENTS

The authors are thankful to Islamic Azad University Science and Research Branch (SRBIAU) and Iran Telecommunication Research Center (ITRC) for bracing this research.

REFERENCES

1. Federal Communication Revision of part 15 of the Commission's Rules Regarding Ultra–Wideband Transmission System, FCC, Washington, DC, 2002, First Report and order FCC, 02. V48.
2. Y. Cho, K. Kim, D. Choi, S. Lee, and S. Park, A miniature UWB planar monopole antenna with 5-GHz band-rejection filter and the time-domain characteristics, IEEE Trans Antennas Propag 54 (2006), 1453–1460.
3. Y. Lee and J. Sun, Proceedings of the 2nd International Conference on Wireless Broadband and Ultra Wideband Communications, 2007, pp.65–69.
4. K. Chung, J. Kim, and J. Choi, Wideband microstrip-fed monopole antenna having frequency band-notch function, IEEE Microw Wirel Compon Lett 15 (2005), 766–768.
5. S. Nikolaou, B. Kim, K. Kim, J. Papapolymerou, and M. Tentzeris, CPW-fed ultra wideband (UWB) monopoles with band rejection characteristic on ultra thin organic substrate, Presented at the Micro. Conference, Asia-pacific, 2006, pp. 2010–2013.
6. Y. Gao, B. Ooi, and A. Popov, Band-notched ultra-wideband ring monopole antenna, Microw Opt Technol Lett 48 (2006), 125–126.
7. K. Kim, Y. Cho, S. Hwang, and S. Park, Band-notched UWB planar monopole antenna with two parasitic patches, IET Electron Lett 41 (2005), 783–785.
8. D.H. Bi and Z.-Y. Yu, Study of dual stopbands UWB antenna with U-slot and V-slot DGS, J Electromagn Wave Appl 22 (2008), 2335–2346.
9. J.-Y. Deng, Y.-Z. Yin, S.-G. Zhou, and Q.-Z. Lin, Compact ultra wideband antenna with tri-band notched characteristic, Electron Lett 44 (2008).
10. S. Nikolaou, N.D. Kingsley, G.E. Ponchak, J. Papapolymerou, and M.M. Tentzeris, UWB elliptical monopoles with a reconfigurable band notch using MEMS switches actuated without bias line, IEEE Trans Antennas Propag 57 (2009), 2242–2250.
11. J. William and R. Nakkeeran, A novel UWB slot antenna with reconfigurable rejection bands, IEICE Electronics Express, 7 (2010), 1515–1519.
12. A.P. Saghati, M. Azarmanesh, and R. Zaker, A novel switchable single- and multifrequency triple-slot antenna for 2.4GHz bluetooth, 3.5GHz WiMax, and 5.8GHz WLAN, IEEE Antennas Wirel Propag Lett 9 (2010).

© 2012 Wiley Periodicals, Inc.

SIMPLE EFFICIENT RESONANT COUPLING WIRELESS POWER TRANSFER SYSTEM OPERATING AT VARYING DISTANCES BETWEEN ANTENNAS

Jongmin Park, Sungho Lee, Youndo Tak, and Sangwook Nam
School of Electrical Engineering and INMC, Seoul National University, Seoul, Korea; Corresponding author: city814@ael.snu.ac.kr

Received 3 January 2012

ABSTRACT: *We found the optimal conditions for an efficient wireless power transfer system (WPTS). In addition, we found that a class-D power amplifier (PA) has an advantage as a source when the input resistance changes with the position of the receiving antenna. Finally, the proposed WPTS was verified through the experimental results.*

© 2012 Wiley Periodicals, Inc.
Microwave Opt Technol Lett 54:2397–2401, 2012; View this article online at wileyonlinelibrary.com. DOI 10.1002/mop.27062

Key words: *near-field coupling*; *wireless power transfer*; *resonant coupling*; *class-DPA*

1. INTRODUCTION

Recently, many groups have reported on a wireless power transfer system (WPTS) that uses resonant coupling [1, 2]. One of the reported issues is the adaptive matching method when the position of the antennas changes. It is known that the optimum impedance vary drastically with the position of the antennas [2]. However, it is difficult to control the source load impedance simultaneously. The authors of Refs. [3–5] suggest the frequency tracking method for adaptive matching. By only controlling the frequency of the source of the WPTS, this method achieves almost simultaneous matching conditions in the strong coupling region. However, this method is limited when applied to a WPTS. In Refs. [3–5], the operating frequency was shifted about 10 to 20 percent from the center frequency. Generally, the relative bandwidth of industrial, scientific, and medical bands are less than 1 percent. Therefore, it is easy to violate the frequency regulation. In this article, we investigated a novel method that achieves efficient wireless power transfer when the operating frequency is fixed and the distance is varied. To do this, the characteristic of the two coupled antennas was analyzed. Then, we took into consideration the types of PA used as a source of the WPTS. The efficiency of PA was analyzed according to the input impedance characteristic of the coupled antennas. Finally, we propose a WPTS, which was verified through experimental results.

2. CHARACTERISTIC OF THE TWO COUPLED ANTENNAS

When two resonant antennas are coupled with each other shown in Figure 1, it can be represented in terms of lumped circuit elements. The equivalent circuit model is shown in Figure 2. The transmitting antenna is expressed by R_{Tx}, L_{Tx}, and C_{Tx}. Like the transmitting antenna, the receiving antenna is also expressed by R_{Rx}, L_{Rx}, and C_{Rx}. In addition, the source resistance is represented by R_{S}. Generally, a WPTS operates at a very low frequency; therefore, the electrical size of the antennas used with a WPTS is very small. Thus, we can assume that the antennas used with a WPTS are quasi-canonical minimum scattering (CMS) antenna. A CMS antenna is defined as one that becomes

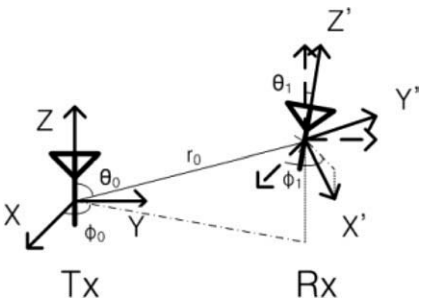

Figure 1 Near-field coupling antennas modeling

invisible when the antenna port is open-circuited [6]. Hence, we set the Z_{11} and Z_{22} as the impedance of the isolated antennas. In addition, electrically small antennas generate mainly the TE_{10} or TM_{10} spherical modes. In addition, antennas that generate the same spherical mode are generally used in a WPTS. Thus, in this article, we assumed that the transmitting and receiving antennas generate a single and identical spherical mode. Generally, a WPTS is used at an electrically close distance. The mutual reactance between the two coupled antennas is dominant compared with the mutual resistance when the antennas are located close enough but are nontouching [2, (56)]. For this reason, the coupling between the antennas is indicated by the mutual reactance X_{21}. In addition, the resonant frequency of the transmitting and receiving antennas is set at the operating frequency of the WPTS; therefore, the impedance of the antennas can be expressed only by the pure resistance component represented by R_{Tx} and R_{Rx}, respectively. From Figure 2, the power transfer efficiency is defined by

$$\mathrm{PTE} = \frac{P_{\mathrm{Load}}}{P_{\mathrm{in}}} = \frac{|i_{\mathrm{Rx}}|^2 R_{\mathrm{Load}}}{|i_{\mathrm{Tx}}|^2 R_{\mathrm{Tx}} + |i_{\mathrm{Rx}}|^2 (R_{\mathrm{Rx}} + R_{\mathrm{Load}})} \tag{1}$$

The relation between the currents of the transmitting and receiving antennas is represented as

$$\frac{i_{\mathrm{Tx}}}{i_{\mathrm{Rx}}} = \frac{R_{\mathrm{Rx}} + R_{\mathrm{Load}}}{jX_{21}}. \tag{2}$$

From Eqs. (1) and (2), the power transfer efficiency is represented as

$$\mathrm{PTE} = \frac{1}{\left(1 + \frac{R_{\mathrm{Rx}}}{R_{\mathrm{Load}}}\right)\left(1 + \frac{R_{\mathrm{Tx}}}{R'_{\mathrm{Load}}}\right)}. \tag{3}$$

R'_{Load} means that the effective load resistance is converted by the mutual impedance. It is represented as

$$R'_{\mathrm{Load}} = \frac{(X_{21})^2}{R_{\mathrm{Rx}} + R_{\mathrm{Load}}}. \tag{4}$$

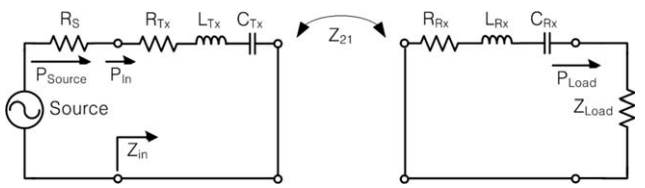

Figure 2 Equivalent circuit of a WPTS

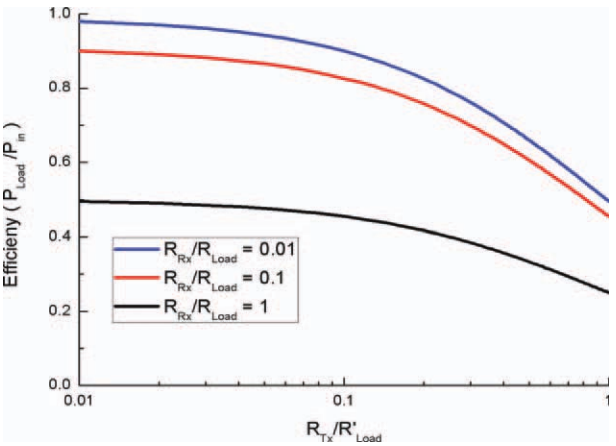

Figure 3 Effect of resistance of antennas and load on the operating power efficiency. [Color figure can be viewed in the online issue, which is available at wileyonlinelibrary.com]

In addition, the optimum load impedance for the maximum power transfer efficiency is represented as

$$R_{\mathrm{Load}}^{\mathrm{opt}} = \sqrt{R_{\mathrm{Rx}}^2 + \frac{R_{\mathrm{Rx}}}{R_{\mathrm{Tx}}}(X_{21})^2}. \tag{5}$$

To maximize the power transfer efficiency, the load resistance must change according to the varied mutual coupling. From Eq. (3), to maximize the power transfer efficiency, the resistances of the antennas, R_{Tx} and R_{Rx}, have to be relatively very small. The condition of the load resistance and the mutual coupling to maximize the power transfer efficiency is represented as

$$R_{\mathrm{Rx}} << R_{\mathrm{load}} << \frac{(X_{21})^2}{R_{\mathrm{Tx}}}. \tag{6}$$

If R_{Tx} is quite small compared with R'_{Load}, the loss at the transmitting antenna can be ignored. Similarly, if R_{Rx} is quite small compared with R_{Load}, the loss at the receiving antenna can be ignored. Consequently, the network of the two coupled antennas works as a quasi-lossless network. The power transfer efficiency according to the ratio of resistance at the transmitting and receiving antennas is shown in Figure 3. The power transfer efficiency increased when the ratio of resistance decreased. According to the goal of power transfer efficiency, the boundary of the ratio of resistance at both antennas can be suggested. From Eq. (6), the condition between the resistance of the antennas and the mutual coupling is represented as

$$R_{\mathrm{Tx}} \cdot R_{\mathrm{Rx}} << (X_{21})^2. \tag{7}$$

When the condition of Eq. (7) is satisfied, the ratio of the resistance is represented as

$$\frac{R_{\mathrm{Rx}}}{R_{\mathrm{Load}}^{\mathrm{opt}}} \approx \frac{R_{\mathrm{Tx}}}{\frac{(X_{21})^2}{R_{\mathrm{Rx}} + R_{\mathrm{Load}}^{\mathrm{opt}}}}. \tag{8}$$

In addition, the maximum efficiency is represented as

$$\mathrm{PTE}_{\mathrm{max}} \approx \frac{1}{\left(1 + \frac{R_{\mathrm{Rx}}}{R_{\mathrm{Load}}^{\mathrm{opt}}}\right)^2}. \tag{9}$$

From Eqs. (7), (9), and [2, (56)], the maximum electrical distance between the antennas is represented as

$$kr_0^{\max} = \begin{cases} \sqrt[6]{\left(\frac{1}{\sqrt{\mathrm{PTE}_{\max}}} - 1\right)^2 \cdot \eta_{\mathrm{Tx}}^{\mathrm{rad}} \cdot \eta_{\mathrm{Rx}}^{\mathrm{rad}} \left[\frac{3}{2}\cos\theta_1(3\cos^2\theta_0 - 1) + \frac{9}{4}\sin\theta_1 \sin\theta_0 \cos(\phi_1 - \phi_0)\right]^2}, & \text{when } \theta_0 \neq \cos^{-1}\left(\frac{1}{\sqrt{3}}\right) \\ \sqrt[6]{\left(\frac{1}{\sqrt{\mathrm{PTE}_{\max}}} - 1\right)^2 \cdot \eta_{\mathrm{Tx}}^{\mathrm{rad}} \cdot \eta_{\mathrm{Rx}}^{\mathrm{rad}} \left[\frac{9}{4}\sin\theta_1 \sin\theta_0 \cos(\phi_1 - \phi_0)\right]^2}, & \text{when } \theta_0 = \cos^{-1}\left(\frac{1}{\sqrt{3}}\right) \text{ and } \theta_1 \neq 0 \text{ and } \phi_1 - \phi_0 \neq \pm\frac{\pi}{2} \\ \sqrt{\left(\frac{1}{\sqrt{\mathrm{PTE}_{\max}}} - 1\right)^2 \cdot \eta_{\mathrm{Tx}}^{\mathrm{rad}} \cdot \eta_{\mathrm{Rx}}^{\mathrm{rad}} \left[\frac{3}{2}\cos\theta_1 \sin^2\theta_0\right]^2}, & \text{when } \theta_0 = \cos^{-1}\left(\frac{1}{\sqrt{3}}\right) \text{ and } \left(\theta_1 = 0 \text{ or } \phi_1 - \phi_0 = \pm\frac{\pi}{2}\right) \end{cases} \quad (10)$$

where η is the radiation efficiency of the antenna. The maximum electrical distance between the antennas is determined by the radiation efficiency of the antennas, the target power transfer efficiency, and the relative location of the receiving antenna. The input resistance at the transmitting antenna is represented as

$$R_{\mathrm{in}} = R_{\mathrm{Tx}} + \frac{(X_{21})^2}{R_{Rx} + R_{\mathrm{Load}}} \quad (11)$$

.

When the distance between the two antennas is varied, the input impedance also changes. Therefore, we need to consider an efficient source type for the WPTS under the condition of varied input impedance.

3. COMPARISON OF SOURCE TYPES

To achieve an efficient WPT system despite the variations in impedance, the characteristic of the PA is such that it is insensitive to load variations. Among various PA types, linear PAs, such as Class-A, B, and AB, have limited efficiency. Thus, nonlinear PAs are preferred in this system due to their high efficiency. In a Class-E PA, the theoretical efficiency is determined by the relationship between the optimum shunt capacitance and load impedance. Thus, the impedance variation can cause sharp degradation in the efficiency [7]. On the contrary, the efficiency of the Class-D PA has a characteristic such that it is insensitive to load variations. The overall efficiency can be sustained over large variations in the load. Therefore, the Class-D PA was selected for the validation of the proposed WPTS. Figure 4 shows the schematic and the efficiency and output power characteristics of the designed class-D amplifier. The input impedance of the measured antenna varied from 4.6 to 400 Ω. It was observed that a high efficiency was maintained over a wide variation in the load resistance.

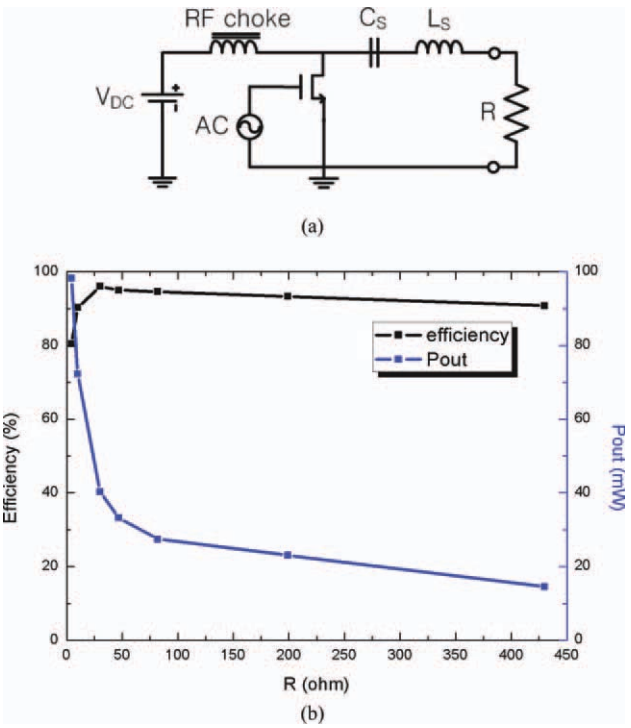

Figure 4 The schematic, efficiency, and output power of PAs against the load resistance: (a) schematic of Class-D PA (V_{DC} = 1V, C_{S} = 58 pF, L_{S} = 15 uH), (b) efficiency and output power. [Color figure can be viewed in the online issue, which is available at wileyonlinelibrary.com]

4. SIMULATION AND MEASUREMENT

To verify this theory, we simulated and measured an actual antenna. We used the commercial software package FEKO. We considered a helix-type loop antenna for the simulation and measurements shown in Figure 5. The two antennas were identical. The simulated resistance of the isolated antenna was 4.1 Ω and the measured resistance of the two isolated antennas was 4.2 and 3.75 Ω, respectively. The radiation efficiency of the antennas was 10^{-4}. A balun efficiency of 95% was used at each antenna. The transmitting and receiving antenna were collinear. The experimental setup is shown in Figure 6. A Class-D PA was used as the source of this system. The delivered power to the load was measured with an oscilloscope. The simulated and measured mutual impedance is shown in Figure 7. As stated above, the mutual reactance was dominant compared to the mutual resistance. From Eq. (11) and Figure 7, the smaller the load resistance was, the larger the input resistance was. The simulated and measured total power transfer efficiency is shown in Figure 8(a). The total power transfer efficiency is represented as

$$\eta_{\mathrm{total}} = \mathrm{PTE} \cdot \eta_{\mathrm{PA}} = \frac{P_{\mathrm{Load}}}{P_{\mathrm{Source}}}. \quad (12)$$

From Eq. (5) and Figure 7, 5, 25, and 68 Ω were the optimum load resistance at 20, 30, and 50 cm, respectively. In addition, only the 25 Ω case satisfied the condition of Eq. (6) between 20

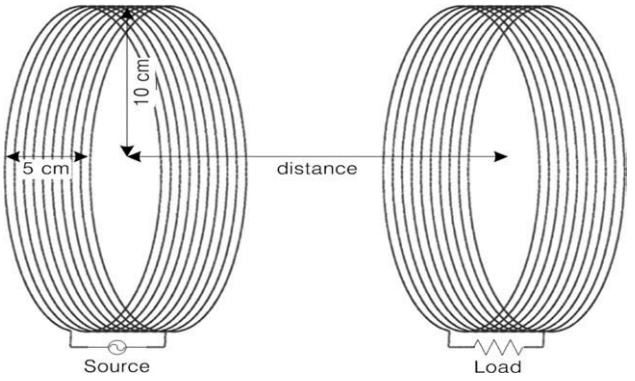

Figure 5 Helix type loop antenna (radius = 10 cm, height = 5 cm, wire thickness = 1 mm, 10 turns, forced resonant frequency = 5.39 MHz)

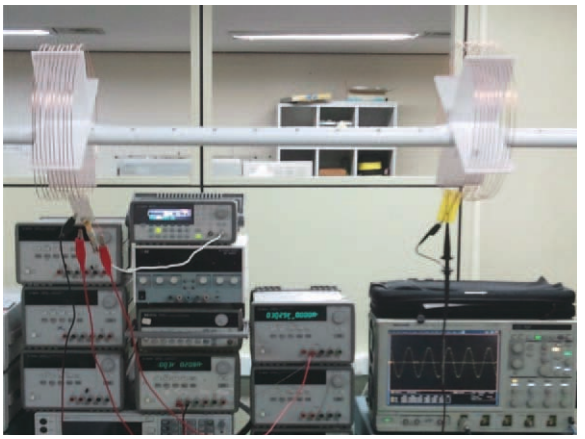

Figure 6 Photograph of the experimental setup of WPTS. [Color figure can be viewed in the online issue, which is available at wileyonlinelibrary.com]

and 30 cm. From Eq. (10), the maximum distance, which guarantees a 70% power transfer efficiency including the balun loss, was about 30 cm. The measured results agreed with the calculated results shown in Figure 8(a). In Figure 8(a), the optimum load impedance case is the maximum power transfer efficiency. When compared with the 5 Ω and 68 Ω cases, the 25 Ω case can efficiently transmit the power at a close distance. There were some differences between the simulated and measured results shown in Figure 8(a). These differences were due to the efficiency of the Class-D PA. From Eq. (11) and Figures 4 and 7, we can infer that the efficiency of the Class-D PA decreases but the output power of the Class-D PA increases when the distance between the antennas is farther apart and the load resistance is bigger. The output power of the Class-D PA and the total power transfer efficiency according to the distance have an opposite trend. The power delivered to the load is shown in Figure 8(b). By only the additional control of the V_{DC} of the Class-D PA, uniform power can be transferred to the load. The proposed WPTS guarantees 70% system efficiency between 20 and 30 cm.

5. CONCLUSION

We investigated a method used to achieve efficient wireless power transfer over a near-field region when the distance between the antennas varied. First, we analyzed the characteristics of two coupled antennas. Then, the conditions that achieve an efficient WPTS for the load resistance and mutual coupling between the antennas were suggested shown in Eq. (6). Then, we compared several types of PAs as a source of the WPTS. The Class-D PA has an advantage in regards to the efficiency of the source for a varied load resistance. The efficiency of the proposed system is almost same to that of the optimum load impedance within a range that satisfies the suggested condition. To realize a WPTS when the coupling between two antennas is varied, our proposed system only needed to control the class-D PA and use a proper load resistance, and as a result, mutual coupling was satisfied (6). Our method is simple when compared with the conditions of other methods when the operating frequency of the WPTS is fixed. Finally, we implemented and tested the proposed WPTS. The experimental results agreed with the simulation results.

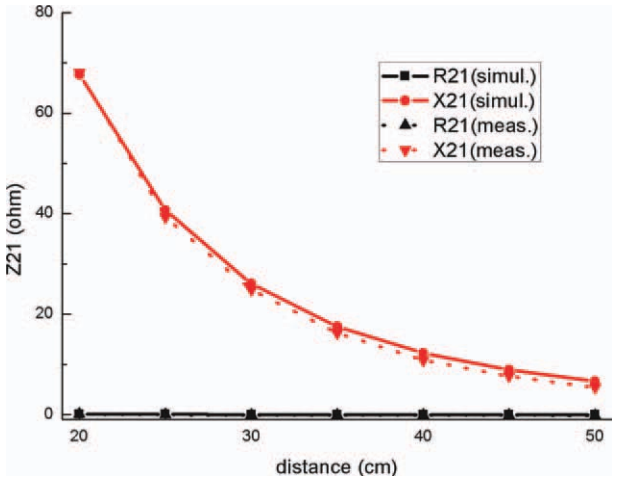

Figure 7 Z_{21} against the distance between the antennas (line: simulated results, dot: measured results). [Color figure can be viewed in the online issue, which is available at wileyonlinelibrary.com]

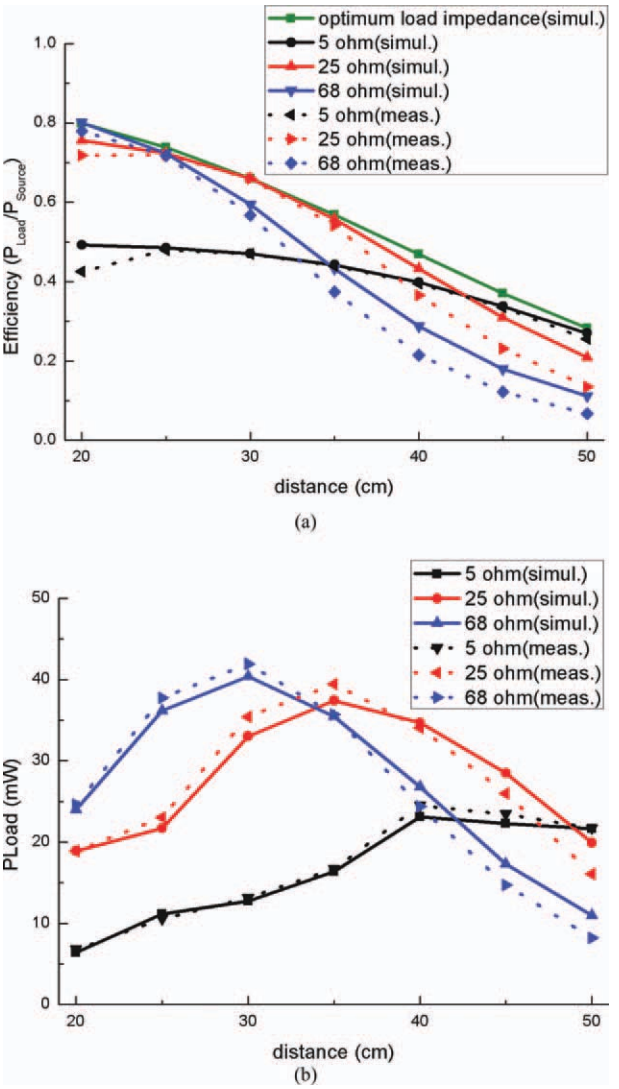

Figure 8 The total power transfer efficiency and output power for two coupled antennas: (a) comparison of the total power transfer efficiency (line: simulated results including the balun loss and assuming that PA efficiency is 100%, dot: the efficiencies are measured results), (b) output power at the load resistance. [Color figure can be viewed in the online issue, which is available at wileyonlinelibrary.com]

ACKNOWLEDGMENTS

This research was supported by the KCC (Korea Communications Commission), Korea, under the R&D program supervised by the KCA (Korea Communications Agency) [KCA-2011-(11911-01110)].

REFERENCES

1. A. Kurs, A. Karalis, R. Moffatt, J.D. Joannopoulos, P. Fisher, and M. Soljacic, Wireless power transfer via strongly coupled magnetic resonances, Science 317 (2007), 83–86.
2. J. Lee and S. Nam, Fundamental aspects of near-field coupling antennas for wireless power transfer, IEEE Trans. Antennas Propag 58 (2010), 3442–3449.
3. Y. Kim and H. Ling, Investigation of coupled mode behaviour of electrically small meander antennas, Electron Lett 43 (2007), 1250–1252.
4. A.P. Sample, D.A. Meyer, and J.R. Smith, Analysis, experimental results, and range adaptation of magnetically coupled resonators for wireless power transfer, IEEE Trans Ind Electron 58 (2011), 544–554.
5. J. Park, Y. Tak, Y. Kim, Y. Kim, and S. Nam, Investigation of adaptive matching methods for near field wireless power transfer, IEEE Trans Antennas Propag 59 (2011).
6. W.K. Kahn and H. Kurss, Minimum-scattering antennas, IEEE Trans Antennas Propag 13 (1965), 671–675.
7. S.C. Cripps, RF power amplifiers for wireless communication, Artech-House, London, 2006, p. 180–199.

© 2012 Wiley Periodicals, Inc.

DESIGN OF A NOVEL ULTRAWIDEBAND ANTENNA WITH DUAL BAND-NOTCHED CHARACTERISTICS

Bin Chen, An-Guo Wang, and Guo-Huang Zhao
School of Electronic Information Engineering, Tianjin University, Tianjin 300072, China; Corresponding author: chenbintju@tju.edu.cn

Received 3 January 2012

ABSTRACT: *A simple printed ultrawideband (UWB) antenna with reconfigurable band-rejected characteristics is proposed. The antenna was fabricated on an FR-4 epoxy substrate and has a volume of 40.0 × 32.0 × 1.0 mm^3. The simulated and measured results show that the antenna has nearly omnidirectional patterns, stable gain, and an available impedance bandwidth of 9.38 GHz which covers 2.34–11.72 GHz. By etching two slots in the radiator, band- notched features centered at 3.5 and 5.5GHz are achieved. With adding two microelectromechanical system switches across slots, the band-rejected characteristics can be reconfigurable and the proposed antenna is capable of operating among none or single or dual band-notched modes. Meanwhile, to discuss the mechanisms of the band-rejected properties, the conceptual equivalent circuit models are presented.* © 2012 Wiley Periodicals, Inc. Microwave Opt Technol Lett 54:2401–2405, 2012; View this article online at wileyonlinelibrary.com. DOI 10.1002/mop.27061

Key words: *band-notched*; *conceptual equivalent circuits*; *microelectromechanical system switch*; *reconfigurable*; *ultrawideband antenna*

1. INTRODUCTION

Since the Federal Communication Commission in United States assigned the spectrum from 3.1 to 10.6 GHz with effective isotropic radiated power less than −41.3 dBm/MHz for unlicensed ultrawideband (UWB) applications in 2002 [1], more and more attention has been drawn on the UWB technology, owing to its especial merits, such as wideband, high speed data rate, high precision ranging, extremely low spectral power density, low cost, and low complexity. As the key components of UWB wireless systems, the UWB antennas also have become one of the hottest research topics. Many types of UWB antenna have been presented, such as biconical, log-periodic, planar monopole antenna, and so on [2]. Among those, printed monopole antenna is the most popular, because of its nearly omnidirectional patterns, small group delay, high radiation efficiency, low profile, easy integration, and stable gain.

Within 3.1–10.6 GHz, there has also existed other allocated wireless bands, such as WiMAX (3.3–3.6 GHz), satellite C-band (3.7–4.2 GHz), and WLAN (5.15–5.825 GHz). To avoid interference effectively and coexist with those wireless communication systems, the band-notched traits are necessary to the designed UWB antennas.

One method to obtain band-rejected functions is to use spatial filter in the antenna [3], but this way will increase cost and easily destroy impedance matching. Another way is to fine-tune configuration to change the state of impedance matching at the desired frequencies. The popular approaches among the second way are inserting slots [4], placing parasitic elements [5], and using defected ground structures [6]. Etching slots is the simplest method, easily achieves band-rejected purposes and has few influences on radiation patterns. In this article, the band-rejected characteristics are obtained by embedding slots in the radiating element. Meanwhile, with adding two simple microelectromechanical system (MEMS) switches on the inserted slots, the dual band-notched traits of proposed antenna can be reconfigurable.

The article is organized as following sections. Section 2 describes the design of the UWB antennas and analyzes the simulated and measured results. Section 3 presents the conceptual equivalent circuit models of the band-notched and reconfigurable band-notched antennas. Section 4 summarizes the study.

2. UWB ANTENNA DESIGN AND RESULTS

2.1. Dual Band-Notched UWB Antenna Design

According to the antenna theory, the size of radiating element can be determined approximately by the empirical formula (1) [7] as follows,

$$f_L = \frac{72}{L + W/2\pi + g} \tag{1}$$

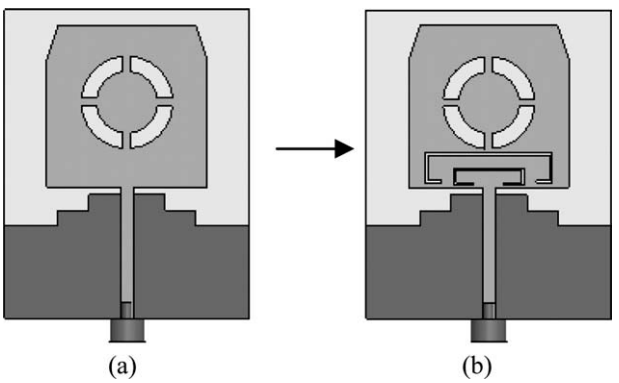

Figure 1 Design evolution of UWB antenna. (a) Antenna I. (b) Antenna II